Available online at www.sciencedirect.com
SCIENCE DIRECT®
Journal of Organometallic Chemistry 666 (2003) 35–42
Journal of Organometallic Chemistry
www.elsevier.com/locate/jorganchem

Synthesis and structures of 3,5-bis(trifluoromethyl)pyrazol derivatives of Rh(I), Ir(I), Pd(II) and Pt(II)

Ziyun Wang, Colin D. Abernethy, Alan H. Cowley, Jamie N. Jones, Richard A. Jones *, Charles L.B. Macdonald, Lilu Zhang

Department of Chemistry and Biochemistry, The University of Texas at Austin, Austin, TX 78712, USA

Dedicated with admiration and affection to Professor Jerry L. Atwood on the occasion of his 60th birthday

Abstract

The reaction of 3,5-$(CF_3)_2$PzLi with $[Rh(COD)Cl]_2$, $IrCl(CO)_3$, $[PdCl(\eta^3\text{-}C_3H_5)]_2$ and $PtCl_2(COD)$ in diethylether solution at 0 °C results in the formation of $[Rh(COD)(\mu\text{-}3,5\text{-}(CF_3)_2Pz)]_2$ (**1**), $[Ir(CO)_2(\mu\text{-}3,5\text{-}(CF_3)_2Pz)]_2$ (**2**), $[Pd(\eta^3\text{-}C_3H_5)(\mu\text{-}3,5\text{-}(CF_3)_2Pz)]_2$ (**3**), and $Pt(COD)(\eta^1\text{-}3,5\text{-}(CF_3)_2Pz)_2$ (**4**), respectively (3,5-$(CF_3)_2$Pz = 3,5-$(CF_3)_2$ pyrazolate; COD = 1,5-cyclooctadiene). Compounds **1**–**3** are dimeric with bridging 3,5-$(CF_3)_2$Pz ligands while **4** is monomeric and features two η^1-3,5-$(CF_3)_2$Pz groups. All compounds have been characterized by spectroscopic methods and their X-ray crystal structures have also been determined.

Keywords: Rhodium; Iridium; Palladium; Platinum; Pyrazolyl derivatives

1. Introduction

A variety of bridging ligands have been widely used in the construction of polymetallic supramolecular complexes [1,2]. For example, bridging ligands based on nitrogen donors such as polyazines can serve as conduits for electron and energy transfer processes [3,4]. Another class of bridging ligands capable of generating supramolecular complexes is based on the pyrazolate (Pz) group. The pyrazolate (Pz) ligand and its substituted analogs are known to form a variety of stable complexes with the platinum group metals [3,4].

Since the bis-CF_3 substituted ligand 3,5-bis(trifluoromethyl)pyrazolate is readily available [5] and should impart increased volatility and novel properties to supramolecular complexes, we investigated its use in the preparation of complexes of the platinum group metals. We describe here the syntheses and structures of four new 3,5-bis(trifluoromethyl)pyrazolate derivatives of Rh, Ir, Pd and Pt. These compounds have also proved to be excellent precursors for the CVD of thin films of the corresponding metals under mild conditions.

2. Results and discussion

2.1. Synthesis of 3,5-bistrifluoromethyl pyrazolate complexes 1–4

The reaction of 3,5-$(CF_3)_2$PzLi with $[Rh(COD)Cl]_2$, $Ir(CO)_3Cl$, $[PdCl(\eta^3\text{-}C_3H_5)]_2$ or $Pt(COD)Cl_2$ in diethylether solution at 0 °C produced the CF_3-substituted pyrazolate derivatives **1**–**4** in good yields (Scheme 1). These compounds are all hydrocarbon soluble and may be readily recrystallized from hexane or hexane–toluene mixtures at −10 to −30 °C.

2.2. $[Rh(COD)(\mu\text{-}3,5\text{-}(CF_3)_2Pz)]_2$ (1)

There are a number of analogs of the rhodium complex **1** known in the literature. These include derivatives of 3,5-dimethyl pyrazolate such as $[(CO)_2Rh(\mu\text{-}3,5\text{-}(Me)_2Pz)]_2$ and $[Rh(COD)(\mu\text{-}3,5\text{-}(Me)_2Pz)]_2$ [6], the fluorinated carbonyl derivative $[Rh(CO)_2(\mu\text{-}3,5\text{-}(CF_3)_2Pz]_2$ [7], and the unsubstituted pyrazolate $[Rh(COD)(\mu\text{-}Pz)]_2$ [8].

The ^{1}H-NMR spectrum of the rhodium complex **1** features five signals that are assigned to the pyrazolate C*H* and COD protons (see Section 3). Each set of

* Corresponding author

0022-328X/02/$ - see front matter
PII: S0022-328X(02)02030-2

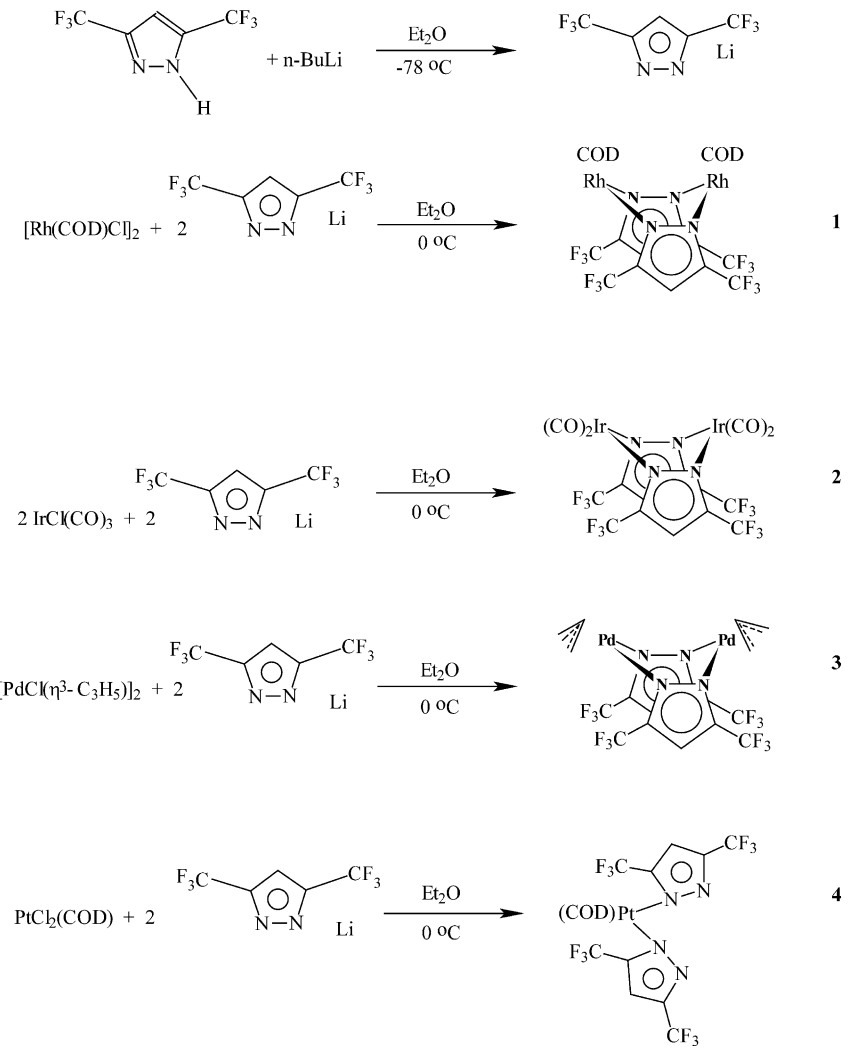

Scheme 1. Synthesis of 3,5-bis(trifluoromethyl)pyrazolate derivatives.

signals for the C*H* and CH_2 protons of COD appear as two resonances. This observation suggests that the structure in solution is similar to that in the solid state with two square planar Rh(I) centers bridged by two $(CF_3)_2$Pz units in a boat-like conformation. The ^{13}C- and ^{19}F-NMR spectroscopic data are also in accord with the X-ray structure.

Compound **1** crystallizes in the orthorhombic space group *Pccn* with four molecules per unit cell. Fig. 1 shows the overall molecular geometry and atom numbering scheme. Crystallographic details are presented in Table 1 and a listing of key bond lengths and angles appears in Table 2. The hydrogen atoms were located and refined isotropically. The overall molecular structure is similar to those of the unsubstituted pyrazolate (Pz) and iridium analogs [Rh(COD)Pz]$_2$ and [Ir(COD)μ-3,5-$(CF_3)_2$Pz)]$_2$ [6]. The central Rh_2N_4 core adopts a boat-like conformation such that the dihedral angle between the two pyrazolate rings is 77.6°. The angle between the planes of the two square planar Rh(I) moieties is 72.2° which may be compared with that found in [Ir(COD)μ-3,5-$(CF_3)_2$Pz]$_2$ of 70.1° [8]. The Rh–Rh distance is 3.164(4) Å which is slightly shorter than that found in the unsubstituted analog [Rh(COD)(Pz)]$_2$ (3.267(2) Å). A slightly larger contraction in metal–metal distance was found in the Ir analogs [Ir(COD)Pz]$_2$ (3.216(1) vs. [Ir(COD)μ-3,5-$(CF_3)_2$Pz]$_2$ (3.073(1) Å) [8]). These differences were attributed to steric factors and it seems likely that this is also the case for **1** and [Rh(COD)Pz]$_2$. Thus the bulky CF_3 substituents force each COD ligand into closer proximity and this change is accompanied by a shortening of the nonbonded, Rh–Rh distance. The other metrical parameters for **1** fall within normal limits.

2.3. [Ir(CO)$_2$(μ-3,5-(CF$_3$)$_2$Pz)]$_2$ (2)

There is a considerable amount of information available in the literature on dinuclear pyrazolate-bridged iridium complexes. Much of this work stems

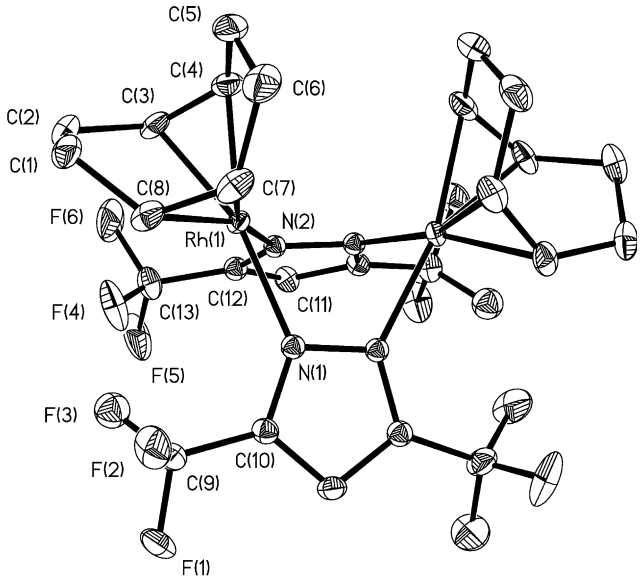

Fig. 1. Molecular structure and atom numbering scheme for $[Rh(COD)(\mu\text{-}3,5\text{-}(CF_3)_2Pz]_2$ (**1**). Thermal ellipsoids are scaled to the 30% probability level. Hydrogen atoms have been omitted for clarity.

Table 2
Selected bond lengths (Å) and angles (°) for **1**

Bond lengths	
C(3)–C(4)	1.392(3)
C(3)–Rh(1)	2.127(2)
C(4)–Rh(1)	2.140(2)
C(7)–Rh(1)	2.138(2)
C(8)–Rh(1)	2.142(2)
N(1)–N(2)#1	1.359(2)
N(1)–Rh(1)	2.1135(18)
N(2)–N(1)#1	1.359(2)
N(2)–Rh(1)	2.1241(17)
Rh(1)–Rh(1)#1	3.1640(12)
Bond angles	
C(10)–N(1)–Rh(1)	138.34(14)
C(12)–N(2)–Rh(1)	134.35(14)
N(1)#1–N(2)–Rh(1)	117.58(12)
N(1)–Rh(1)–N(2)	83.94(6)
N(1)–Rh(1)–C(3)	161.23(8)
N(2)–Rh(1)–C(3)	89.55(8)
N(1)–Rh(1)–C(7)	92.61(8)
N(2)–Rh(1)–C(7)	164.72(8)
N(1)–Rh(1)–C(4)	160.31(8)
N(2)–Rh(1)–C(4)	97.07(8)
N(1)–Rh(1)–C(8)	97.50(8)
N(2)–Rh(1)–C(8)	157.37(8)
C(3)–Rh(1)–C(8)	81.91(9)

from the pioneering studies of Atwood and coworkers [8,9]. Thus both the CF_3-substituted and unsubstituted iridium analogs of **2**, $[Ir(COD)(\mu\text{-}3,5\text{-}(CF_3)_2Pz)]_2$ and $[Ir(COD)(\mu\text{-}Pz)]_2$ are known and have been structurally characterized [8]. As noted above, the Rh analog of **2** is known [7] as well as other methyl-substituted iridium analogs [10]. However, to the best of our knowledge, the fluorinated carbonyl derivative $[Ir(CO)_2(\mu\text{-}3,5\text{-}(CF_3)_2Pz)]_2$ (**2**), has not yet been reported.

The spectroscopic data for **2** are consistent with the X-ray structure analysis (Fig. 2). Thus the ^{1}H-NMR spectrum consists of a single sharp line at δ 6.12 and the IR spectrum contains three intense peaks in the ν_{CO}

Table 1
Crystallographic data for compounds **1**–**4**

	1	**2**	**3**	**4**
Empirical formula	$C_{26}H_{26}F_{12}N_4Rh_2$	$C_{14}H_2F_{12}Ir_2N_4O_4$	$C_{16}H_{12}F_{12}N_4Pd_2$	$C_{36}H_{24}F_{24}N_8Pt_2$
Formula weight	828.33	902.60	701.10	1414.81
Temperature (K)	198(2)	293(2)	293(2)	213(2)
Space group	*Pccn*	$P2_12_12_1$	$P2_1/c$	$P2_1/c$
Unit cell dimensions				
a (Å)	10.503(5)	9.0728(4)	9.3641(2)	17.700(5)
b (Å)	14.326(5)	12.4732(6)	18.2139(5)	13.401(5)
c (Å)	18.872(5)	19.1065(4)	13.4544(3)	18.481(5)
α (°)	90	90	90	90
β (°)	90	90	104.802(1)	104.600(5)
γ (°)	90	90	90	90
V (Å^3)	2839.6(18)	2162.2(2)	2218.59(9)	4242.1(3)
Z	4	4	4	4
D_{calc} (g cm^{-3})	1.938	2.773	2.099	2.215
Absorption coefficient (mm^{-1})	1.267	12.430	1.732	6.735
Reflections observed [$I > 2\sigma(I)$]	3238	4777	2829	3557
Final R indices [$I > 2\sigma(I)$] [a]	$R_1 = 0.0243$, $wR_2 = 0.0563$	$R_1 = 0.0310$, $wR_2 = 0.0764$	$R_1 = 0.0279$, $wR_2 = 0.0546$	$R_1 = 0.0692$, $wR_2 = 0.1714$
R indicies (all data) [a]	$R_1 = 0.0272$, $wR_2 = 0.0579$	$R_1 = 0.0349$, $wR_2 = 0.0785$	$R_1 = 0.0620$, $wR_2 = 0.0596$	$R_1 = 0.0835$, $wR_2 = 0.2090$
Largest difference peak and hole (e Å^{-3})	1.284 and 0.950	2.574 and −2.321	0.775 and −0.573	3.871 and −5.858

[a] $R_1 = \Sigma_{hkl}\ (||F_o| - |F_c||)/\Sigma_{hkl}|F_o|$. $R_2 = [\Sigma\ w(|F_o| - |F_c|)^2/\Sigma\ w|F_o|^2]^{1/2}$.

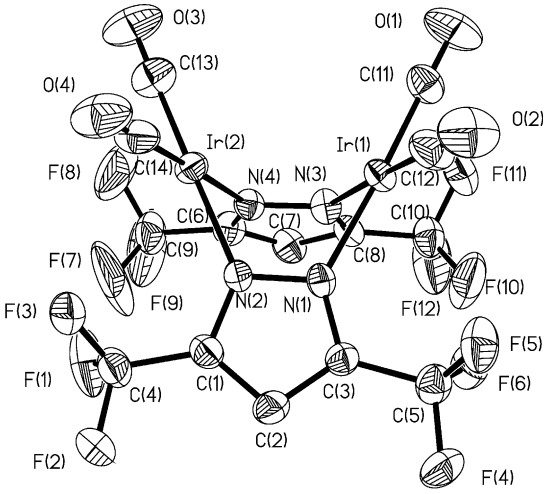

Fig. 2. Molecular structure and atom numbering scheme for $[Ir(CO)_2(\mu\text{-}3,5\text{-}(CF_3)Pz)]_2$ (**2**). The thermal ellipsoids are scaled at the 30% probability level.

stretching region (2104, 2082 and 2036 cm^{-1}). A similar pattern is evident in the IR spectrum of the rhodium analog $[Rh(CO)_2\mu\text{-}3,5\text{-}(CF_3)_2Pz]_2$ ($\nu_{co} = 2100$, 2090 and 2050 cm^{-1}).

Compound **2** crystallizes in the orthorhombic space group $P2_12_12_1$ with four molecules per unit cell. As in the case of **1**, the molecular structure of **2** has a boat-like conformation with a dihedral angle between the two Ir(I) planes of 69.2°. The non-bonding Ir–Ir distance is 3.122(4) Å, which may be compared with that found in the parent complex $[Ir(COD)Pz]_2$ (3.216(1) Å) [7]. Key bond lengths and angles for **2** are listed in Table 3.

Table 3
Selected bond lengths (Å) and angles (°) for **2**

Bond lengths	
Ir(1)–C(11)	1.857(8)
Ir(1)–C(12)	1.863(9)
Ir(1)–N(1)	2.081(5)
Ir(1)–N(3)	2.092(6)
Ir(1)–Ir(2)	3.1217(4)
Ir(2)–C(14)	1.852(9)
Ir(2)–C(13)	1.857(9)
Ir(2)–N(2)	2.069(6)
Ir(2)–N(4)	2.083(6)
N(2)–N(1)	1.342(8)
N(4)–N(3)	1.343(9)
Bond angles	
C(11)–Ir(1)–C(12)	89.3(4)
C(11)–Ir(1)–N(1)	176.8(3)
C(12)–Ir(1)–N(1)	93.1(3)
C(11)–Ir(1)–N(3)	94.0(3)
C(12)–Ir(1)–N(3)	176.6(3)
N(1)–Ir(1)–N(3)	83.5(2)
C(11)–Ir(1)–Ir(2)	112.5(3)
C(12)–Ir(1)–Ir(2)	113.9(3)
N(1)–Ir(1)–Ir(2)	64.58(15)
N(3)–Ir(1)–Ir(2)	64.7(2)
C(14)–Ir(2)–C(13)	90.7(4)
C(14)–Ir(2)–N(2)	92.8(3)
C(13)–Ir(2)–N(2)	176.4(3)
C(14)–Ir(2)–N(4)	176.3(3)
C(13)–Ir(2)–N(4)	93.0(3)
N(2)–Ir(2)–N(4)	83.5(2)
C(14)–Ir(2)–Ir(1)	113.1(3)
C(13)–Ir(2)–Ir(1)	114.3(3)
N(2)–Ir(2)–Ir(1)	64.63(15)
N(4)–Ir(2)–Ir(1)	64.8(2)

2.4. $[Pd(\eta^3\text{-}C_3H_5)(\mu\text{-}3,5\text{-}(CF_3)_2Pz)]_2$ (**3**)

The reaction of $[PdCl(\eta^3\text{-}C_3H_5)]_2$ with two equivalents of $3,5\text{-}(CF_3)_2PzLi$ in diethylether solution yields the dimeric complex $[Pd(\eta^3\text{-}C_3H_5)(\mu\text{-}3,5\text{-}(CF_3)_2Pz)]_2$ (**3**) in high yield. At room temperature the ^{1}H-NMR spectrum of **3** exhibits seven sets of multiplets (see Section 3), that are assigned to the η^3-allyl groups, in addition to three peaks at δ 6.50, 6.52 and 6.55, that are attributed to the single hydrogen of the bis(trifluoromethyl)pyrazolate ligand. The ^{19}F-NMR spectrum of **3** features two broad resonances at δ −59.94 and −59.87. At low temperature (−70 °C) in d_8-toluene, the peaks broaden considerably. These data suggest that in solution there is a mixture of isomers. Of relevance here is the original series of dinuclear palladium(II) allyl derivatives of dimethylpyrazolate or of the parent pyrazolate reported by Trofimenko in 1971 [6]. For these compounds it was also found that the ^{1}H-NMR spectra were more complex than those anticipated for a molecule with simple C_{2v} symmetry. It was proposed that the NMR data were compatible with a mixture of conformational isomers resulting from the rotation of the allyl groups, inversion of the entire metallocycle, or the presence of isomer (I) (Fig. 3).

In 1977, Henslee and Oliver [11] reported the X-ray crystal structure of the dimethyl pyrazolate derivative $[Pd(\eta^3\text{-}C_3H_5)(\mu\text{-}3,5\text{-}Me_2Pz)]_2$. In the solid state this compound has a symmetrical structure in which both allyl groups point inwards towards the center of the

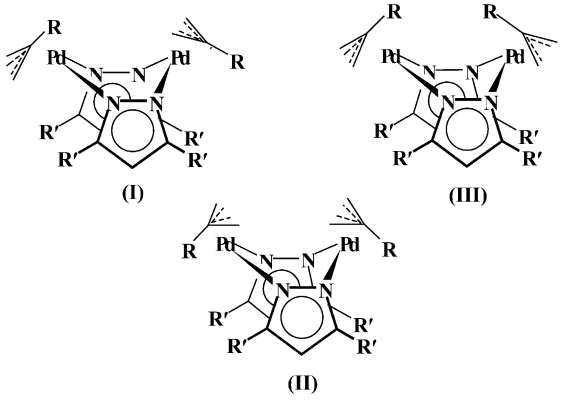

Fig. 3. Conformational isomers possible for Pd complexes from Ref. [6].

Pd_2N_4 core. This configuration is represented by isomer (II) (Fig. 3). Interestingly, the solid state structure of **3** corresponds to the conformational isomer (I)—as originally proposed by Trofimenko for the other pyrazolate derivatives [6].

In the solid state **3** crystallizes in the monoclinic space group $P2_1/c$ with four independent molecules in the unit cell (Fig. 4). Key bond lengths and angles are presented in Table 4. As observed in the structures of **1** and **2** the pyrazolate ligands in **3** give the central core of the molecule a boat-like configuration. The geometry about each Pd(II) atom is approximately square planar with the angle between the centroids of each alkyl unit of 107.5°.

The metrical parameters associated with the central $Pd_2(\mu\text{-}3,5\text{-}(CF_3)_2Pz)_2$ core in **3** are similar to those in $[Pd(\eta^3\text{-}C_3H_5)(\mu\text{-}3,5\text{-}Me_2Pz)]_2$ [11]. Thus the Pd–Pd distance in **3** is 3.2169(4) Å compared with 3.343 Å in the case of dimethyl derivative. In both compounds the two Pd–N–N–Pd planes intersect at similar angles (103.2(5)° in **3** and 106.6° in the dimethyl compound). The Pd–N bond lengths in **3** range from 2.101(3) to 2.111(3) Å and are thus slightly longer than those found in the dimethyl derivative (2.067(7)–2.083(7) Å). The Pd–C bond lengths fall within the range 2.099(4)–2.133(4) Å. However, they do not appear to follow a regular pattern in which the terminal carbon atoms of the π-allyl groups have longer Pd–C distances than those of the central carbon atoms. A similar trend was observed in the case of $[Pd(\eta^3\text{-}C_3H_5)(\mu\text{-}3,5\text{-}Me_2Pz)]_2$.

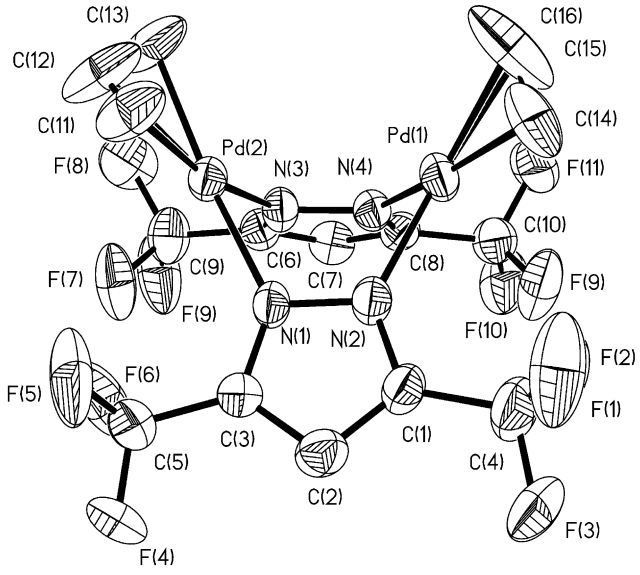

Fig. 4. Molecular structure and atom-numbering scheme for $[Pd(\eta^3\text{-}C_3H_5)(\mu\text{-}3,5\text{-}(CF_3)_2Pz)]_2$ (**3**). The thermal ellipsoids are scaled to the 30% probability level, and hydrogen atoms have been omitted for clarity.

Table 4
Selected bond lengths (Å) and angles (°) for **3**

Bond lengths	
Pd(1)–N(4)	2.101(3)
Pd(1)–C(15)	2.104(6)
Pd(1)–N(2)	2.111(3)
Pd(1)–C(16)	2.124(4)
Pd(1)–C(14)	2.133(4)
Pd(1)–Pd(2)	3.2169(4)
Pd(2)–C(13)	2.099(4)
Pd(2)–C(12)	2.103(5)
Pd(2)–N(3)	2.108(3)
Pd(2)–N(1)	2.109(3)
Pd(2)–C(11)	2.130(4)
Bond angles	
N(4)–Pd(1)–C(15)	133.6(2)
N(4)–Pd(1)–N(2)	89.67(10)
C(15)–Pd(1)–N(2)	134.1(2)
N(4)–Pd(1)–C(16)	99.9(2)
C(15)–Pd(1)–C(16)	37.3(2)
N(2)–Pd(1)–C(16)	170.3(2)
N(4)–Pd(1)–C(14)	169.4(2)
C(15)–Pd(1)–C(14)	37.5(2)
N(2)–Pd(1)–C(14)	100.7(2)
C(16)–Pd(1)–C(14)	69.6(2)
N(4)–Pd(1)–Pd(2)	63.22(8)
C(15)–Pd(1)–Pd(2)	116.8(3)
N(2)–Pd(1)–Pd(2)	63.51(7)
C(16)–Pd(1)–Pd(2)	122.2(2)
C(14)–Pd(1)–Pd(2)	123.6(2)
C(13)–Pd(2)–C(12)	36.4(2)
C(13)–Pd(2)–N(3)	100.7(2)
C(12)–Pd(2)–N(3)	135.2(2)
C(13)–Pd(2)–N(1)	166.8(2)
C(12)–Pd(2)–N(1)	135.5(2)
N(3)–Pd(2)–N(1)	89.17(10)
C(13)–Pd(2)–C(11)	68.8(2)
C(12)–Pd(2)–C(11)	36.4(2)
N(3)–Pd(2)–C(11)	168.0(2)
N(1)–Pd(2)–C(11)	100.5(2)
C(13)–Pd(2)–Pd(1)	112.1(2)
C(12)–Pd(2)–Pd(1)	130.6(2)
N(3)–Pd(2)–Pd(1)	64.46(7)
N(1)–Pd(2)–Pd(1)	64.17(7)
C(11)–Pd(2)–Pd(1)	113.3(2)

2.5. $Pt(COD)(\eta^1\text{-}3,5\text{-}(CF_3)_2Pz)_2$ (**4**)

The reaction of $PtCl_2(COD)$ with two equivalents of $3,5\text{-}(CF_3)_2PzLi$ in diethylether solution at 0 °C results in good yields of monomeric $Pt(COD)(\eta^1\text{-}3,5\text{-}(CF_3)_2Pz)_2$ (**4**). Although it has been noted recently that η^1-binding for the pyrazolate ligand is less common than the bridging mode [12,13], several examples of Pt complexes with η^1-pyrazolate ligands have been reported. These include analogs of **4** based on chelating diphosphines [14] or bipyridyl [15] with either the pyrazolate or 3,5-dimethylpyrazolate ligands. In addition, Fackler et al. have also reported the synthesis and structural characterization of the mono pyrazolate derivative, $(PPh_3)_2ClPt(3,5\text{-}Ph_2Pz)$ [16].

The spectroscopic data for **4** are consistent with the presence of a monomer in solution that features two η^1-bonded 3,5-$(CF_3)_2$Pz ligands. The $^{19}F\{^1H\}$-NMR spectrum of **4** is particularly informative since it shows two simple sharp peaks that are assignable to CF_3 groups in two different environments.

In the solid state **4** crystallizes in the monoclinic space group $P2_1/c$ (Fig. 5). Key bond lengths and angles are given in Table 5. There are two pairs of independent molecules per unit cell and they have similar structural parameters. The coordination geometry about Pt(1), which comprises the centroids of the C=C bonds of COD and the two N atoms, is close to square planar. The largest deviation from planarity is 0.971 Å and the sum of the angles about Pt(1) is 345°. The angle subtended by the two pyrazolate nitrogens bonded to Pt(1) is 92.6(7)° (N(38)–Pt(1)–N(47)). The two pyrazolate units are orientated such that the intramolecular interactions between CF_3 groups are minimized. Hence the uncoordinated pyrazolate nitrogen atoms are directed away from each other. The dihedral angle between the two pyrazolate rings is 83.95(5) (molecule 1) and 83.1(5)° (molecule 2). The Pt–N bond lengths of 2.014(18) and 2.060(17) Å in **4** (molecule 2) are slightly longer than those found in the bipyridyl analog (4,4′-dimethyl-2,2′-bipyridyl)bis(3,5-dimethylpyrazolate)platinum(II) (average 1.983(7) Å) [15]. The other metrical parameters for **4** fall within normal limits and are unexceptional.

Preliminary studies have shown that **1**–**4** are useful precursors for the CVD of the respective metals under relatively mild conditions [17]. Comprehensive CVD and materials characterization studies are in progress and will be the subject of a future publication.

Table 5
Selected bond lengths (Å) and angles (°) for one molecule of **4**

Bond lengths	
Pt(1)–N(38)	2.014(18)
Pt(1)–N(47)	2.060(17)
Pt(1)–C(7)	2.12(2)
Pt(1)–C(16)	2.16(2)
Pt(1)–C(11)	2.204(17)
Pt(1)–C(131)	2.20(2)
C(7)–C(16)	1.40(3)
C(7)–C(14)	1.52(3)
N(38)–C(63)	1.37(3)
N(38)–N(58)	1.39(2)
N(47)–N(55)	1.32(2)
N(47)–C(51)	1.36(3)
Bond angles	
N(38)––Pt(1)–N(47)	92.6(7)
N(38)–Pt(1)–C(7)	164.5(7)
N(47)–Pt(1)–C(7)	86.2(8)
N(38)–Pt(1)–C(16)	157.4(7)
N(47)–Pt(1)–C(16)	92.5(7)
C(7)–Pt(1)–C(16)	38.0(8)
N(38)–Pt(1)–C(11)	87.9(7)
N(47)–Pt(1)–C(11)	164.8(6)
C(7)–Pt(1)–C(11)	97.3(8)
C(16)–Pt(1)–C(11)	81.6(7)
N(38)–Pt(1)–C(131)	94.5(8)
N(47)–Pt(1)–C(131)	156.6(7)
C(70–Pt(1)–C(131)	81.1(8)
C(16)–Pt(1)–C(131)	89.5(8)
C(11)–Pt(1)–C(131)	38.1(7)
C(16)–C(7)––C(14)	128(2)
C(16)–C(7)–Pt(1)	72.8(13)
C(14)–C(7)–Pt(1)	109.9(13)

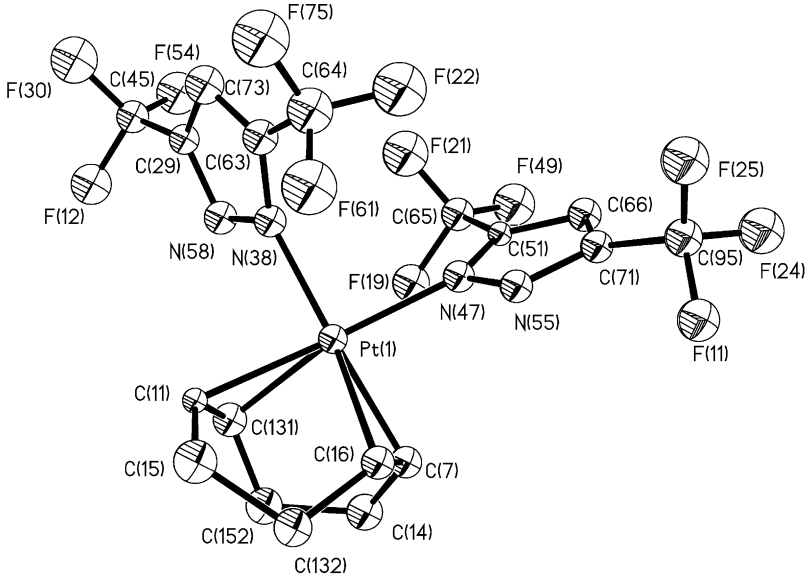

Fig. 5. Molecular structure and atom-numbering scheme for one molecule of Pt(COD)(η^1-3,5-$(CF_3)_2$Pz)$_2$ (**4**). The thermal ellipsoids have been scaled to the 30% probability level and hydrogen atoms have been omitted for clarity.

3. Experimental

3.1. General data

All reactions were performed under a dry, oxygen-free nitrogen atmosphere or under vacuum using standard Schlenk line and dry box techniques. All solvents were dried prior to use by distillation from molten sodium or sodium benzophenone ketyl under nitrogen. 3,5-Bis(trifluoromethyl)pyrazole [5], $[Rh(COD)Cl]_2$ [18], IrCl(CO) [19], $[ClPd(\eta^3\text{-}C_5H_5)]_2$ [20], and $PtCl_2(COD)$ [21] were prepared as described in the literature.

NMR measurements were made at room temperature (r.t.) on a General Electric QE 300 (^1H, 300 MHz; ^{13}C, 75 MHz; ^{19}F, 282 MHz) spectrometer. The chemical shifts are reported in ppm with positive values corresponding to downfield shifts from the standard. Proton chemical shifts are reported relative to tetramethylsilane (Me_4Si, $\delta = 0.00$) and are referenced to the residual protons of C_6D_6 (^1H, $\delta = 7.15$; ^{13}C, $\delta = 128.0$).

IR measurements were made as Nujol mulls between KBr plates on a Digilab FTS-40 spectrometer. Elemental analyses were performed by Atlantic Microlab, Norcross, GA. High and low resolution mass spectra were obtained with a VG Analytical ZAB2-E mass spectrometer in the chemical ionization mode with CH_4 as the ionizing gas.

3.2. X-ray structure determinations

X-ray data were collected using a Siemens P4 diffractometer equipped with a Nicolet LT-2 low temperature device and using a graphite monochromator with Mo–K_α radiation ($\lambda = 0.71073$ Å). Data were collected in the ω-scan mode. Details of crystal data, data collection and structure refinements are listed in Table 1. Data reduction, decay and absorption corrections, structure solution and refinements were performed using the SHELXTL/PC software package [22]. The structures were solved by direct methods and refined by full-matrix least-squares on F^2 with anisotropic displacement parameters for the non-H atoms. Neutral atom scattering factors and values used to calculate the linear absorption coefficient are taken from the International Tables for X-ray Crystallography (1992) [23].

3.3. Synthesis of $[Rh(COD)(\mu\text{-}3,5\text{-}(CF_3)_2Pz)]_2$ (1)

A solution of *n*-BuLi (1.3 ml, 1.6 M) in C_6H_{14} was added to a solution of 3,5-$(CF_3)_2$PzH (0.41 g, 2.02 mmol) in Et_2O (30 ml) at −78 °C. This solution was stirred for a further 30 min and then added dropwise to a solution of $[Rh(COD)Cl]_2$ (0.50 g, 1.01 mmol) in Et_2O at 0 °C. The resulting reaction mixture was stirred overnight at r.t. then filtered through a short bed of Celite®. The filtrate was evaporated to dryness under vacuum and the residue recrystallized from a C_6H_{14}–$C_6H_5CH_3$ mixture at −10 °C. For **1**: m.p. 243–245 °C. Isolated yield: 0.56 g, 67%. ^1H-NMR (300 MHz, C_6D_6): δ 6.34 s(pyrazolate C*H*, 1H), 4.79 (s, C*H*, 2H), 4.21 (s, C*H*, 2H), 2.49 (m, CH_2, 4H), 1.66 (m, CH_2, 4H); $^{13}C\{^1H\}$ (C_6D_6): δ 30.3 (s, CH_2), 31.2 (s, CH_2), 81.1 (s, *C*H), 83.3 (s, *C*H), 107.5 (s, *C*H, Pz) 121.3 (q, $^1J = 262.5$ Hz, CF_3), 143.4 (q, $^2J = 30$Hz, *C*–CF_3, Pz); ^{19}F-NMR (C_6D_6): δ −57.4 (C_6F_6 reference); MS *m/e*: 828 [M^+], 809 [$M^+ - F$]; Anal. Found: C, 38.92; H, 3.30; N, 6.85. Calc.: C, 37.7; H, 3.16; N, 6.76%.

3.4. Synthesis of $[Ir(CO)_2(\mu\text{-}3,5\text{-}(CF_3)_2Pz)]_2$ (2)

A solution of *n*-BuLi (1.14 ml, 1.6 M) in C_6H_{14} was added to a solution of 3,5-$(CF_3)_2$PzH (0.36 g, 1.80 mmol) in Et_2O (25 ml) at −78 °C. This solution was stirred for further 30 min and then added dropwise to a solution of $IrCl(CO)_3$ (0.56 g, 1.80 mmol) in Et_2O (10 ml) at 0 °C. The resulting reaction mixture was stirred for 12 h at r.t., then filtered through a bed of Celite®. The filtrate was evaporated to dryness under vacuum and the residue recrystallized from C_6H_{14} (−30 °C). For **2**: m.p. 120–122 °C. Isolated yield: 0.61 g, 75%. ^1H-NMR (300 MHz, C_6D_6): δ 6.12; $^{13}C\{^1H\}$-NMR (C_6D_6): δ 107.8, 119.7 (q, $^1J = 270.0$ Hz), 143.5 (q, $^2J = 40.0$ Hz); ^{19}F-NMR (C_6D_6): δ −58.4 (C_6F_6 as reference); FT-IR (C_6H_{14}), $\nu_{co} = 2036$, 2082, 2104 cm^{-1}; MS *m/e*: 902 [M^+], 883 [$M^+ - F$]; Anal. Found: C, 18.87; H, 0.30; N, 6.29. Calc. for $C_{14}H_2F_{12}Ir_2N_4O_4$: C, 18.63; H, 0.22; N, 6.21%.

3.5. Synthesis of $[Pd(\eta^3\text{-}C_3H_5)(\mu\text{-}3,5\text{-}(CF_3)_2Pz)]_2$ (3)

A solution of *n*-BuLi (2.06 ml, 1.6 M) in C_6H_{14} was added to a solution of 3,5-$(CF_3)_2$PzH (0.6 g, 3.28 mmol) in Et_2O (25 ml) at −78 °C. This solution was stirred for a further 30 min and then added dropwise to a solution of $[PdCl(\eta^3\text{-}C_3H_5)]_2$ (0.60 g, 1.64 mmol) in Et_2O (20 ml) at 0 °C. The resulting reaction mixture was stirred at r.t. for 12 h, then filtered through a bed of Celite®. The filtrate was evaporated to dryness under vacuum and the residue recrystallized from C_6H_{14} at −30 °C. For **3**: m.p. 220–222 °C. Isolated yield: 0.98 g, 85%. ^1H-NMR (C_6D_6): δ 2.39 (d, 1H, $^1J = 12.6$ Hz), 2.40 (d, 1H, $^1J = 12.6$ Hz), 2.81 (d, 1H, $^1J = 12.6$ Hz), 2.85 (d, 1H, $^1J = 12.6$ Hz), 3.55 (d, 1H, $^1J = 7.0$ Hz), 3.58 (d, 1H, $^1J = 7.0$ Hz), 3.77 (d, 1H, $^1J = 7.0$ Hz), 3.81 (d, 1H, $^1J = 7.0$ Hz), 4.72 (septet, 0.5H, $^1J = 7.0$ Hz), 4.83 (septet, 0.5H, $^1J = 7.0$ Hz), 5.05 (m, 1H), 6.50, 6.52, 6.55; $^{13}C\{^1H\}$-NMR (C_6D_6): δ 59.3, 59.8, 60.4, 60.6, 114.5, 114.8, 115.8, 116.3, 121.2 (q, $^1J = 269$ Hz), 121.23 (q, $^1J = 269$ Hz), 121.4 (q, $^1J = 269$ Hz), 121.43 (q, $^1J = 269$ Hz), 142.82 (q, $^2J = 38$ Hz), 142.90 (q, $^2J = 38$ Hz), 143.12 (q, $^2J = 38$ Hz), 143.22 (q, $^2J = 38$ Hz); ^{19}F-NMR (C_6D_6): δ −59.94, −59.87. MS *m/e*: 700 [M^+], 682 [M−F]; Anal. Found: C, 27.5; H, 1.73; N, 7.98. Calc. for $C_{16}H_{12}F_{12}N_4Pd_2$: C, 27.4; H, 1.73; N, 7.99%.

3.6. Synthesis of $Pt(COD)(\eta^1\text{-}3,5\text{-}(CF_3)_2Pz)_2$ (4)

A solution of *n*-BuLi (2.0 ml, 1.6 M) in C_6H_{14} was added to a solution of 3,5-$(CF_3)_2$PzH (0.64 g, 3.2 mmol) in Et_2O (30 ml) at −78 °C. This solution was stirred for a further 30 min and then added dropwise to $PtCl_2$(COD) (0.60 g, 1.6 mmol) in Et_2O (20 ml) at 0 °C. The resulting reaction mixture was stirred at r.t. for 12 h, then and filtered through a bed of Celite®. The filtrate was evaporated to dryness under vacuum and the residue recrystallized from C_6H_{14}–$C_6H_5CH_3$ (−30 °C). For **4**: m.p. 134–136 °C. Isolated yield: 0.85 g, 75%. ^{1}H-NMR ($CDCl_3$): δ 2.35 (s, 3H), 2.58 (m, 4H), 2.88 (m, 4H), 5.86 (s, br, 4H), 6.73 (s, 2H), 7.16–7.25 (m, 4H); $^{13}C\{^1H\}$-NMR ($CDCl_3$): δ 21.5, 30.3, 105.1, 106.0, 120.3 (q, $^1J = 269$ Hz), 121.5 (q, $^1J = 269$ Hz), 125.4, 128.3, 129.1, 138.0, 139.8 (q, $^2J = 38$ Hz), 144.1 (q, $^2J = 37$ Hz); ^{19}F-NMR ($CDCl_3$): δ −59.5, −61.4; MS *m/e*: 709 [M^+]; Anal. Found: C, 31.0; H, 2.14; N, 7.86. Calc. for $C_{18}H_{14}F_{12}N_4Pt$: C, 30.4; H, 1.97; N, 7.90%.

4. Supplementary material

Crystallographic data for the structural analysis have been deposited with the Cambridge Crystallographic Data Center, CCDC nos. 192833, 192830, 192831, and 192832 for compounds **1**, **2**, **3**, and **4**, respectively. Copies of this information may be obtained free of charge from The Director, CCDC, 12 Union Road, Cambridge CB2 1EZ, UK (Fax: +44-1223-336033; e-mail: deposit@ccdc.ac.uk or www: http://www.ccdc.cam.ac.uk).

Acknowledgements

We thank the Robert A. Welch Foundation (Grants F-816 and F-135) and the Science and Technology Center Programs of the National Science Foundation (Grant No. CHE 08920120) for partial support of a postdoctoral position (Z.W.).

References

[1] J.L. Atwood, et al., Comprehensive Supramolecular Chemistry, Pergammon, Oxford, vol. 9, 1996, p. 213.
[2] See for example: S. Swavey, Z. Fang, K.J. Brewer, Inorg. Chem. 41 (2002) 2598.
[3] A.P. Sadimenko, S.S. Basson, Coord. Chem. Rev. 147 (1996) 247.
[4] G. La Monica, G.A. Ardizzoia, Prog. Inorg. Chem. 46 (1997) 151.
[5] O. Renn, L.M. Venanzi, A. Marteletti, V. Gramlich, Helv. Chim. Acta 78 (1995) 993.
[6] S. Trofimenko, Inorg. Chem. 10 (1971) 1372.
[7] G. Banditelli, A.L. Bandini, E. Bonati, G. Minghetti, J. Organomet. Chem. 218 (1981) 229.
[8] K.A. Beveridge, G.W. Bushnell, S.R. Stobart, J.L. Atwood, M.J. Zaworotko, Organometallics 2 (1983) 1447.
[9] G.W. Bushnell, D.O. Kimberly Fjeldsted, S.R. Stobart, M.J. Zaworotko, S.A.R. Knox, K.A. Macpherson, Organometallics 4 (1985) 1107.
[10] J.L. Marshall, M.D. Hopkins, V.V. Miskowski, H.B. Gray, Inorg. Chem. 31 (1992) 5034.
[11] G.W. Henslee, J.D. Oliver, J. Cryst. Mol. Struct. 7 (1977) 137.
[12] See for example: (a) W. Zheng, H.W. Roesky, M. Nolte-Meyer, Organometallics 20 (2001) 1033;
(b) D. Carmona, J.L. Fernando, L.A. Oro, Organometallics 10 (1991) 3123;
(c) A.I.P.G. Yap, C.H. Winter, Inorg. Chem. 36 (1997) 1738;
(d) P. Legzdins, S.J. Rettig, K.M. Smith, V. Tong, G.V. Young, J. Chem. Soc. Dalton Trans. (1997) 3269;
(e) J. Campora, J.L. Lopez, M.C. Maya, P. Palma, E. Carmona, Organometallics 19 (2000) 2707.
[13] See for example: (a) J.R. Perera, M.J. Heeg, H.B. Schlegel, C.H. Winter, J. Am. Chem. Soc. 121 (1999) 4536;
(b) J.E. Cosgriff, G.B. Deacon, Angew. Chem. Int. Ed. Engl. 37 (1988) 286 and references therein.
[14] G. Minghetti, G. Banditelli, F. Bonati, Dalton Trans. (1979) 1851.
[15] W.P. Schaeffer, W.B. Connick, U.M. Miskowski, H.B. Gray, Acta Crystallogr. Sect. C 48 (1992) 1776.
[16] J.P. Fackler, R.G. Raptis, H.H. Murray, Inorg. Chem. Acta 193 (1992) 173.
[17] Y.M. Sun, private communication.
[18] G. Giordano, R.H. Crabtree, Inorg. Synth. 19 (1979) 218.
[19] A.P. Ginsberg, J.W. Koepke, C.R. Sprinkle, Inorg. Synth. 19 (1979) 18.
[20] Y. Tatsuno, T. Yoshida, S. Tsuka, Inorg. Synth. 19 (1979) 220.
[21] D. Drew, J.R. Doyle, Inorg. Synth. 13 (1972) 48.
[22] G.M. Sheldrick, SHELXTL/PC (Version 5.03), Siemens Analytical X-ray Instruments, Inc., Madison, WI, USA, 1994.
[23] International Tables for X-ray Crystallography, vol. C, Tables 4.2.6.8 and 6.1.1.4, A.J.C. Wilson (Ed.), Kluwer Academic Press, Boston, 1992.